Processing – morphology – property relationships of polyamide 6/polyethylene blend–clay nanocomposites

R. Scaffaro[*], *L. Botta, M. C. Mistretta, F. P. La Mantia*

Dipartimento di Ingegneria Civile, Ambientale, Aerospaziale, dei Materiali, Università di Palermo, Viale delle Scienze, Ed. 6, 90128 Palermo, Italy

Abstract. In this work, we studied the effect of the method of preparation and of reprocessing on the morphology and, consequently, on the physical properties of polyamide 6 (PA6)/ high density polyethylene (HDPE)-clay nanocomposite blends in the presence of different compatibilizers. In particular, the nanocomposites were obtained by melt mixing using a co-rotating twin screw extruder (E1). The blends thus obtained were re-extruded (E2) under the same operating conditions. Moreover, blends with the same final composition were produced using a masterbatch of the compatibilizer with the clay prepared in a separated stage in a batch mixer (MB). All the materials were characterized by scanning electron microscopy (SEM), transmission electron microscopy (TEM) and X-ray diffractometry (XRD) analyses. In addition, the rheological behaviour and the, tensile and impact, properties were evaluated. The XRD and TEM analysis showed that re-extrusion slightly improves the morphology of the nanocomposites. A further improvement of the morphology, in terms of lower clay dimension and better dispersion, was observed in the MB blends. The results of the mechanical tests showed that reprocessing (E2) induced an increase of all the properties for all the three systems. A further general increase of the mechanical properties was showed by the MB blends.

Keywords: nanocomposites, organoclay, compatibilization, polymer blends

1. Introduction

There are several studies on the preparation and the properties of nanocomposites based on polymer blends in the presence or not of compatibilizers [1–9].

Blends of polyamides with polyolefins and polyesters are particularly interesting and attractive from an industrial point of view. During the last years, it has been shown that such blends can be efficiently compatibilized with numerous compounds derived from maleic anhydride, acrylic acid, glycidyl methacrylate, oxazoline, etc., grafted onto the polyolefin chain so that hydrogen bonds, or even covalent bonds, can be formed between the two polymers at the blending stage [10–18].

Nanocomposites based on polyethylene (PE) and polyamide (PA) blends have also been studied. In particular, the effect of the composition and of filler level was investigated [19–24]. In our previous works we presented the properties of high density polyethylene (HDPE) and polyamide 6 (PA6) blends containing an organically modified montmorillonite (OMM) [25, 26]. We evaluated the effect of different compatibilizing systems on the properties of the blends. The results indicated that, despite a good morphology achieved in the filled blends and a moderate intercalation level, the mechanical performance, especially the properties at break, were not satisfactory. This behaviour was attributed to degradation phenomena involving the organic modifier of the clay that were reduced by using a stabi-

---

lizing system. These degradation phenomena were deeply investigated in other works [27, 28]. We studied the effect of thermal treatments under different atmospheres and for different times on the behaviour of organically modified clays, demonstrating that the degradation products of the modifier (α-olefins transforming into various carboxyl compounds if oxygen is present) initially increased the basal spacing, followed by a collapse of the particle layers when the decomposition products migrated toward the surface and eventually volatilized. Moreover, in order to understand the possible different interactions of neat and degraded modified clay, composites were prepared in the melt and fully characterized.

There are several works regarding the effect of reprocessing on the morphology and on the properties of polymer based nanocomposites, but to the best of our knowledge no similar studies was performed on nanocomposite based on polymer blends [29–34].

Aim of this work is to evaluate the influence of morphology, at nano and micro scale, achieved by different processing methods on the rheological and mechanical properties of blends of PA6/HDPE in the presence of OMM and different compatibilizing systems. The morphology of the blends was studied by XRD, TEM and SEM analyses.

2. Experimental section
2.1. Materials and pre-treatments
The PA6 used in this work was a sample of Radilon S35 100 NAT, kindly supplied by Radicinova, Italy. It has an intrinsic viscosity (measured in sulfuric acid) equal to 3.4 dL/g. The HDPE was an injection moulding grade (MP94, Polimeri Europa, Italy, Melt Flow Index at 190°C/2,16 kg = 7 g/10 min).

Three compatibilizing systems were used in this work: an ethylene-co-acrylic acid copolymer (EAA) (Escor 5001, Exxon chemical, acrylic acid content 6.2 wt%) together with a 2,2′-(1,3-phenylene)-bis(2-oxazoline) (PBO) (1,3-PBO, Adeka Palmarole, melting point 146°C); a high-density polyethylene modified with acrylic acid (HDAA) (Polybond 1009, Chemtura, acrylic acid content 6 wt%) together
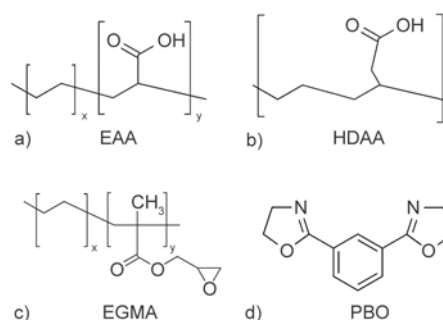
Figure 1. Chemical structure of each compatibilizer used in this work: a) EAA; b) HDAA, c) EGMA, d) PBO

with PBO and an ethylene-co-glycidyl methacrylate copolymer (EGMA) (Lotader AX8840, Arkema, glycidyl methacrylate content 8 wt%). The chemical structure of each compatibilizer is reported in the Figure 1.

Nanocomposites were prepared by adding 5 phr of montmorillonite modified with alkylammonium salts (Cloisite 15A, Southern Clay). The organic modifier is a dimethyl-ditallow, with two organophilic tails fully hydrogenated with an average composition of 65% C_{18}, 30% C_{16} and 5% C_{14}.

Prior to processing, all the materials, except PBO and HDPE used as-received, were dried in order to prevent hydrolytic scission of the polyamide. PA6 was dried for 10 h in a ventilated oven at 90°C followed by 16 h under vacuum at 120°C, while EAA, HDAA and EGMA were dried for 3 h under vacuum at 70°C and the Cloisite was dried 12 h under vacuum at 120°C.

2.2. Processing
Blends PA6/HDPE 25/75 w/w were produced by using a co-rotating modular twin screw extruder (OMC, Italy). All the blends prepared together with sample code and composition are reported in Table 1. The materials were prepared using different procedures as reported in Table 2. Some blends were prepared by premixing all the components in the solid state and then feeding them all together into the extruder (E1). The thermal profile was 180–200–210–220–230–240–240°C and the screw speed 220 rpm. Under these conditions, the residence time, measured by feeding a colour tracer to the extruder

Table 1. Sample code and composition of the blends prepared in the present work

Code sample	PA6	HPDE	EAA	HDAA	EGMA	PBO	CL15A
PA6/HDPE/EAA/PBO/15A	25	75	5	–	–	0.2	5
PA6/HDPE/HDAA/PBO/15A	25	75	–	5	–	0.2	5
PA6/HDPE/EGMA/15A	25	75	–	–	5	–	5

Table 2. Sample code of different preparation method

Code sample	Processing
PA6/HDPE/EAA/PBO/15A/E1	Extrusion
PA6/HDPE/HDAA/PBO/15A/E1	Extrusion
PA6/HDPE/EGMA/15A/E1	Extrusion
PA6/HDPE/EAA/PBO/15A/E2	Re-Extrusion
PA6/HDPE/HDAA/PBO/15A/E2	Re-Extrusion
PA6/HDPE/EGMA/15A/E2	Re-Extrusion
PA6/HDPE/EAA/PBO/15A/MB	Masterbatch
PA6/HDPE/HDAA/PBO/15A/MB	Masterbatch
PA6/HDPE/EGMA/15A/MB	Masterbatch

in a separated test, was about 80 s. The molten material coming out from the extruder die was immediately cooled on line in a water bath, pelletized and then used for further characterization. In another procedure, part of the pelletized blends was further re-extruded adopting the same conditions in order to evaluate the effect of the re-processing (E2). In another procedure, blends with the same final composition were prepared using a masterbatch of the compatibilizer (EAA, HDAA or EGMA) with Cloisite 15A, prepared in a separated stage at 180°C and 64 rpm in a Brabender batch mixer. In particular, the masterbatch and the other components of the blends were premixed in the solid state and fed to the extruder adopting the same conditions reported above (MB).

2.3. Characterization

The morphology of the clay and of the nanocomposites was evaluated by using X-ray diffractometry (XRD), scanning electron microscopy (SEM) and transmission electron microscopy (TEM). XRD analyses were performed using a diffractometer Siemens D-500 in reflection mode with an incident X-ray wavelength of 0.1542 nm. The morphology of the samples was analyzed by a scanning electron microscope (SEM) (Quanta 200F ESEM, FEI, USA). All samples were fractured in liquid nitrogen and sputter-coated with a thin layer of gold to avoid electrostatic charging under the electron beam. Transmission electron microscopy (TEM) images were obtained with a Philips EM 208 TEM with 100 keV accelerating voltage. Ultrathin sections (50 nm thickness) of the specimens, cooled at ; 80°C, were obtained by cryo-ultramicrotomy with a diamond knife cooled at –60°C.

Rheological measurements were carried out using a parallel plate rheometer (RDAII, Rheometrics) equipped with plates of 25 mm diameter in dynamic

mode. The testing temperature was 240°C and the frequency range 0.1–500 rad/s.

Mechanical characterization was carried out on specimens cut off from compression-moulded sheets ($10 \times 90 \times {\sim}0.6$ mm). Mechanical testing was performed using an Instron 4443 tensile testing machine according to ASTM D882. The grip distance was 50 mm and the crosshead speed was 50 mm/min. IZOD impact test were carried out using a CEAST 6545/000 according with ASTM D256 on notched specimens.

All the specimens for the mechanical and rheological characterization were prepared by compression moulding at 240°C using a Carver Laboratory press (100 bar, 7 min) on materials dried for 3 h at 120°C in a vacuum oven.

3. Results and discussion
3.1. X-ray diffractometry (XRD)

In order to evaluate the morphology of OMM after processing, XRD diffraction has been carried out on all the samples. In Figure 2, there are reported the XRD patterns of blends compatibilized with EAA, Figure 2a, HDAA, Figure 2b and EGMA, Figure 2c, prepared by single extrusion (E1), re-extrusion (E2) and extrusion with a masterbatch (MB). As reported in our previous works, the XRD pattern of Cloisite 15A (here not reported for sake of clarity) presents a main broad peak at 2.8° (the position is indicated with dotted vertical lines included in Figure 2a–2c) corresponding to a d-spacing of 3.15 nm [26, 35–37]. In Table 3 there are reported the values of 2θ corresponding to the main diffraction peak of the XRD patterns and the respective values of interlayer distance calculated by Bragg's law.

As regards all the blends, it is worth observing that they all present peaks associated to the clay. This feature suggests that an exfoliated structure was never achieved at least under the processing and composition conditions here adopted.

In all compatibilized blends E1 the peak related to Cloisite 15A shifted towards lower angles and, as reported in Table 3, therefore the d-spacing increased. In accordance with our previous work, this is particularly true for the blend compatibilized with EAA/PBO system as the interlayer distance is above 4 nm [26]. The structure achieved by the organoclay in the compatibilized blends can be explained considering that, on increasing the compatibilizing effect, the adhesion between the different phases and the
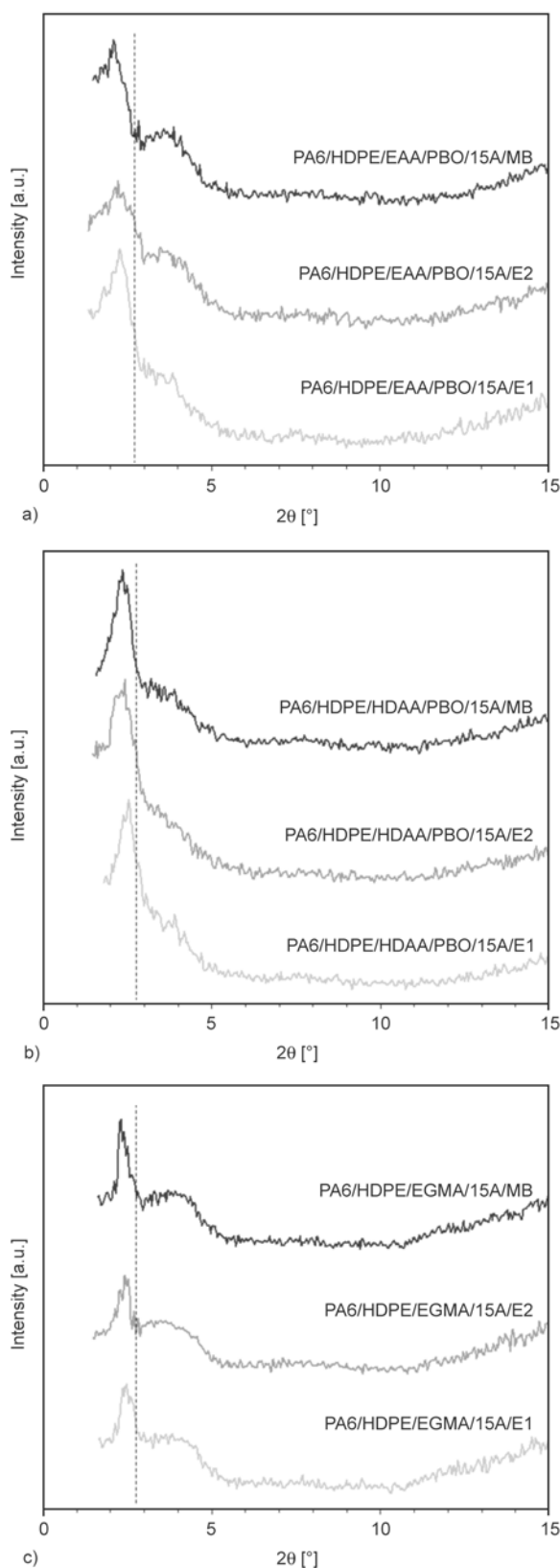
Figure 2. XRD patterns of blends compatibilized with a) EAA, b) HDAA and c) EGMA prepared by single extrusion (E1), re-extrusion (E2) and extrusion with a masterbatch (MB). The dotted vertical lines indicates the position corresponding to main peak at 2.8° of neat Cloisite 15A

Table 3. Interlayer distance of neat CL15A and of compatibilized blends prepared by single extrusion (E1), re-extrusion (E2) and extrusion with a masterbatch (MB)

Sample	2θ [°]	d-spacing [nm]
CL 15A as received	2.80	3.15
PA6/HDPE/EAA/PBO/15A/E1	2.20	4.02
PA6/HDPE/EAA/PBO/15A/E2	2.14	4.13
PA6/HDPE/EAA/PBO/15A/MB	2.07	4.27
PA6/HDPE/HDAA/PBO/15A/E1	2.48	3.56
PA6/HDPE/HDAA/PBO/15A/E2	2.38	3.72
PA6/HDPE/HDAA/PBO/15A/MB	2.31	3.83
PA6/HDPE/EGMA/15A/E1	2.40	3.68
PA6/HDPE/EGMA/15A/E2	2.39	3.70
PA6/HDPE/EGMA/15A/MB	2.25	3.93

melt stresses, are increased. As a consequence, the clay tactoids are more stressed and the polymer chains can enter the galleries thus increasing the d-spacing [26].

The XRD spectra of the re-extruded blends (E2) show that both in the system containing EAA, Figure 2a, and in that containing HDAA, Figure 2b, the peak related to Cloisite 15A shifts to lower angles. Indeed, as reported in Table 3, the interlayer distance of the clay incorporated in the polymer matrix increases after the reprocessing growing from 4.02 to 4.13 nm for the EAA compatibilzed blends and from 3.56 to 3.72 nm for blends containing HDAA. Such result, according to the scientific literature, can be likely ascribed to the supplementary stresses induced on the blend by the second processing. This would allow a further dispersion/redistribution of the nanofiller with consequent higher intercalation level [32–34].

As regards the EGMA compatibilized materials, Figure 2c, the position of the peak identifying Cloisite 15A remains practically unchanged after the reprocessing and consequently the d-spacing is almost the same for both the samples, i.e. 3.68 nm for PA6/HDPE/EGMA/15A/E1 and 3.70 nm for PA6/HDPE/EGMA/15A/E2.

When a compatibilizer-clay masterbatch is used, there is always a shift of the peak of Cloisite toward angles even lower than those observed for E1 and E2 materials, thus indicating a higher interlayer distance as highlighted by the values of d-spacing reported in Table 3. Indeed, for each compatibilized system the MB blend exhibits the higher interlayer distance.

These results, in accordance with the literature, can be explained considering that the preparation of the

compatibilizer-clay masterbatch may induce a certain initial intercalation/expansion of the clay that becomes more intense during the subsequent extrusion processing [38].

Moreover, the differences observed between the different compatibilizers could depend on their different viscosity and affinity with the nanofiller. This feature, indeed, may cause higher or lower pre-intercalation of the compatibilizer during the masterbatch preparation. HDAA, in fact, having a lower viscosity if compared with the other compatibilizers as reported in our previous work, could be less

effective in dispersing the clay compared with EAA or EGMA [26]. Of course, the affinity between the clay and the compatibilizer plays also a key role in determining the final morphology in the masterbatch and a dedicated study to go deeper inside these aspects will be object of a future work.

3.2. Transmission electron microscopy (TEM)

To better understand the structure of the nanocomposites and to corroborate the conclusions achieved by XRD analysis,, TEM analysis was carried out on the nanocomposites.
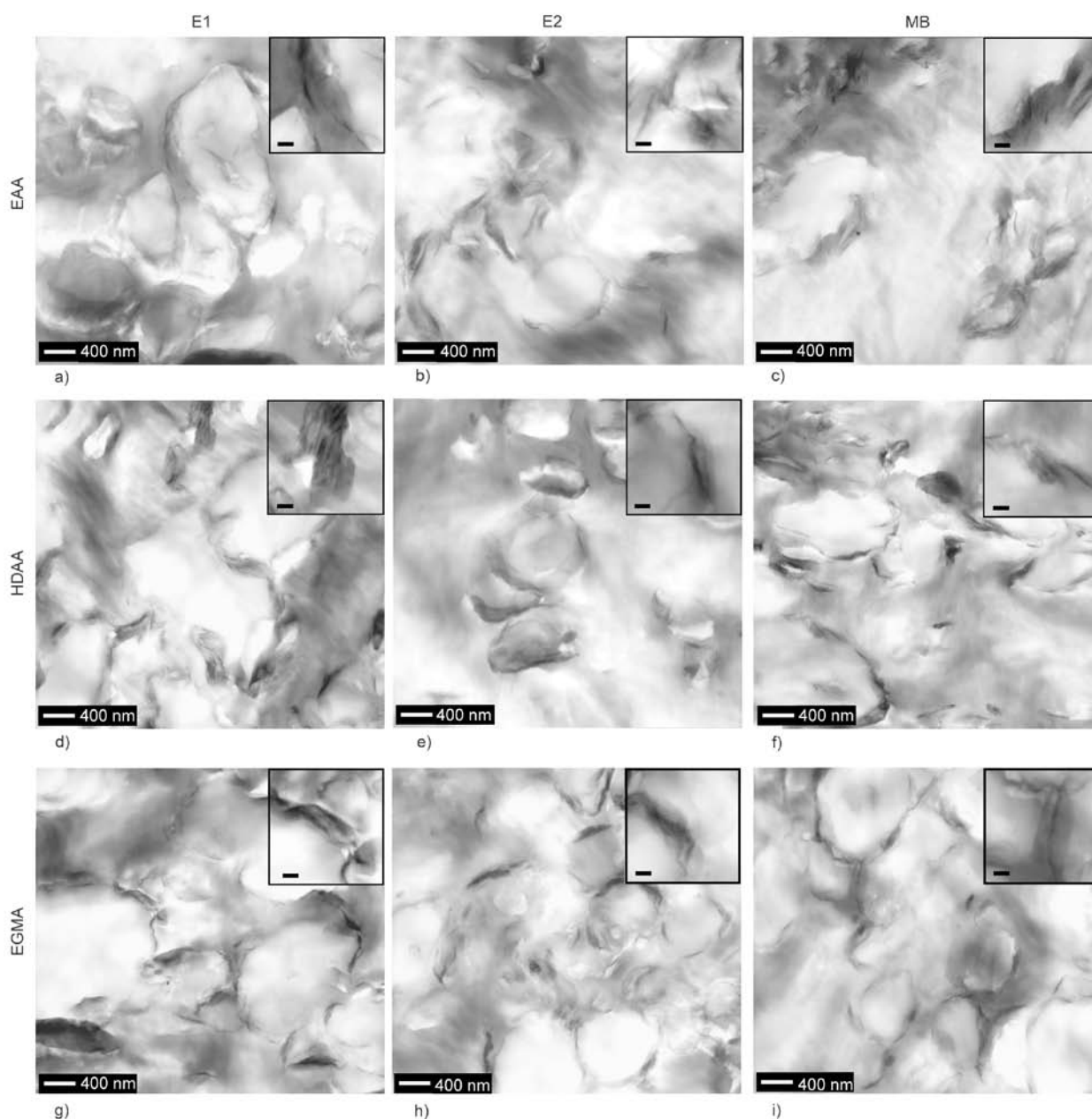
Figure 3. TEM micrographs of compatibilized blends prepared by single extrusion (E1: a, d, g), re-extrusion (E2: b, e, h) and extrusion with a masterbatch (MB: c, f, i). Each TEM image contains inside a frame with the magnification of a illustrative particular. The scale bar contained in each frame corresponds to 100 nm.

In Figure 3 the TEM micrographs of blends compatibilized with EAA, Figure 3a–3c, HDAA, Figure 3d-f, and EGMA, Figure 3g–3i prepared by single extrusion (E1), re-extrusion (E2) and extrusion with a masterbatch (MB) are reported. Each image contains inside a frame with the magnification of an illustrative part.

The TEM micrographs of blends E1 show that the clay in all the materials is mainly organized in intercalated tactoids although some isolated exfoliated silicate sheet can be found. Moreover, it is interesting to note that, despite PA6 is the minor polymeric phase, the filler is mainly located inside the PA6 phase and at HDPE/PA6 interface. This is in agreement with the observation of other authors on similar systems and can be reasonably explained considering that, despite the presence of the organic modifier, the clay is essentially a polar component that, therefore, tends to migrate to the polar part of the blend [39].

In the re-processed materials, it is possible to individuate areas in which the clay tactoids are smaller than those observed in the same non-reprocessed blends. This is particularly true for the blends containing EAA and HDAA as compatibilizers, Figure 3b and 3e. This is in agreement with the XRD analysis and confirms that the second processing helps in dispersing the nanofiller inside the matrix achieving a better morphology.

A further improvement of the morphology, in terms of lower clay dimension and better dispersion, can be observed in the blends prepared using the compatibilizer-clay masterbatch prepared in a separated step prior extruding, Figure 3c , 3f and 3i. Also this result is fully according with the XRD analysis, confirming the positive effects of this procedure on the intercalation/exfoliation of the clay.

3.3. Scanning electron microscopy (SEM)

Differently from TEM that observes very small portions of the material, SEM analysis is a powerful characterization to investigate the overall phase morphology of the polymer blends and of the related composites. In particular, it is possible to evaluate the interfacial modification in the presence of compatibilizers, the dispersion of the phases and the
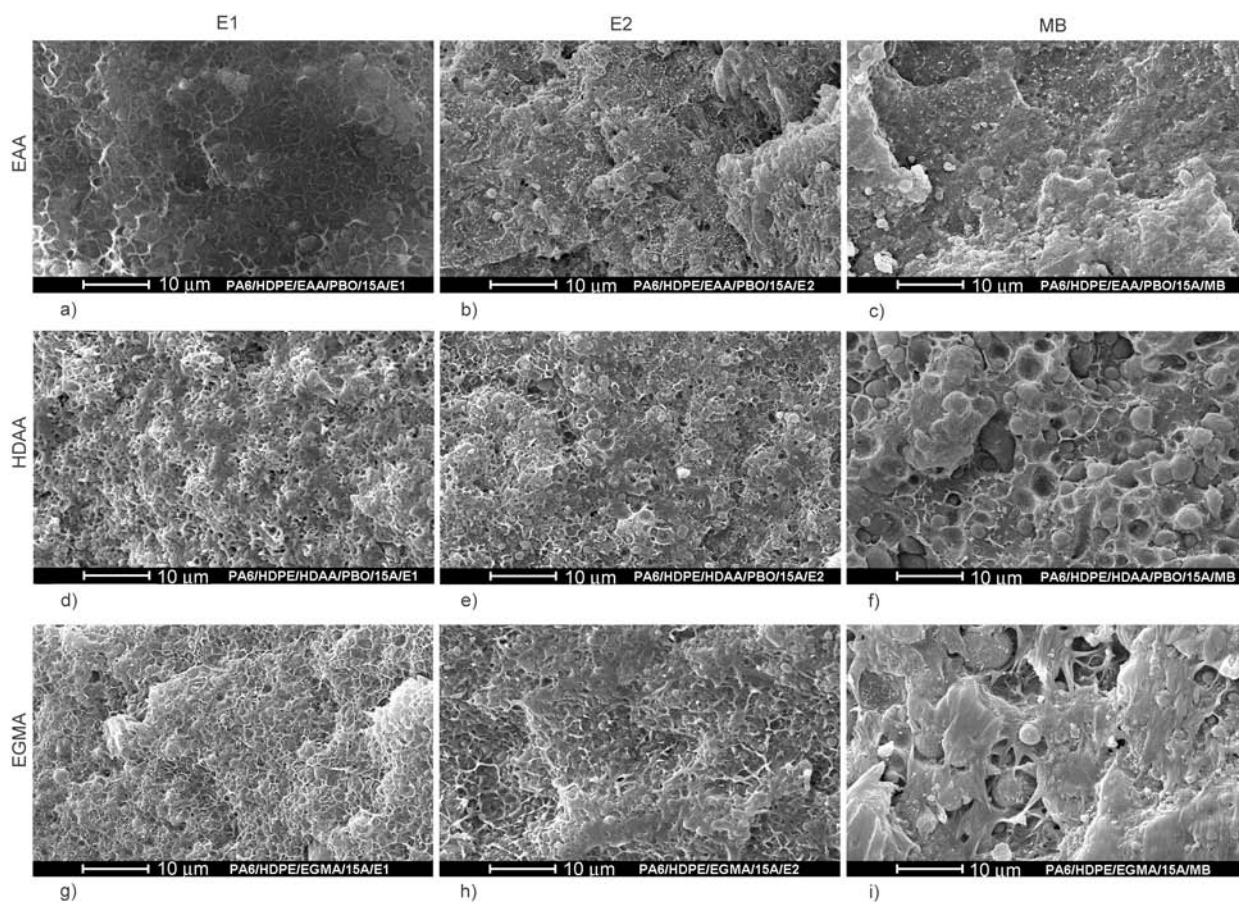
Figure 4. SEM micrographs of compatibilized blends prepared by single extrusion (E1: a, d, g), re-extrusion (E2: b, e, h) and extrusion with a masterbatch (MB: c, f, i)

reciprocal adhesion achieved by different processing methods, with particular reference to the two polymeric phases constituting the matrix.

In Figure 4 there are reported the SEM micrographs of blends compatibilized with EAA, Figure 4 a–4c, HDAA, Figure 4d–4f, and EGMA, Figure 4g–4i prepared by single extrusion (E1), re-extrusion (E2) and extrusion using a clay/compatibilizer masterbatch (MB).

It is evident that in the blends PA6/HDPE/EAA/PBO/15A/E2, Figure 4b, and PA6/HDPE/EAA/PBO/15A/MB, Figure 4c, the dimension of the particles of the PA6 dispersed phase is definitely smaller and the interfacial adhesion better than those observed in the corresponding E1 blend, Figure 4a. It is also possible to see smaller aggregates with a different contrast, ascribable to the clay tactoids, well dispersed both in E1, in E2 and in MB materials.

When using HDAA as compatibilizer, the dimension of the particles of E2, Figure 4e, and especially of MB materials, Figure 4f, is higher if compared with that of E1, Figure 4d. However, the adhesion of E2 seems to be the best. Also in this case, it is possible to find small clay aggregates, better dispersed in E2 and MB materials.

The situation is similar for the EGMA compatibilized blends. In this case, the blends E2, Figure 4h and MB, Figure 4i, display a rougher morphology if compared with E1, Figure 4g, but the adhesion of the former is definitely better, as the particles are well embedded in the matrix. It is worth noting that the dispersion of the clay aggregates is here less uniform if compared with that observed in the materials compatibilized with EAA/PBO or HDAA.

### 3.4. Rheological characterization

The complex viscosity, the storage modulus and the loss modulus as a function of frequency are reported in Figure 5–7 for all the materials.

As regards the blends compatibilized with the EAA/PBO system, Figure 5, the viscosity of PA6/HDPE/EAA/PBO/15A/E2 is the lowest of this series of materials while E1 and MB show almost the same values. This can be likely interpreted with degradation phenomena occurring during the second reprocessing. It must be highlighted that, from one side, reprocessing can absolutely improve the overall morphology, especially in terms of dimension. Nevertheless, it cannot be disregarded that in E2 blends,
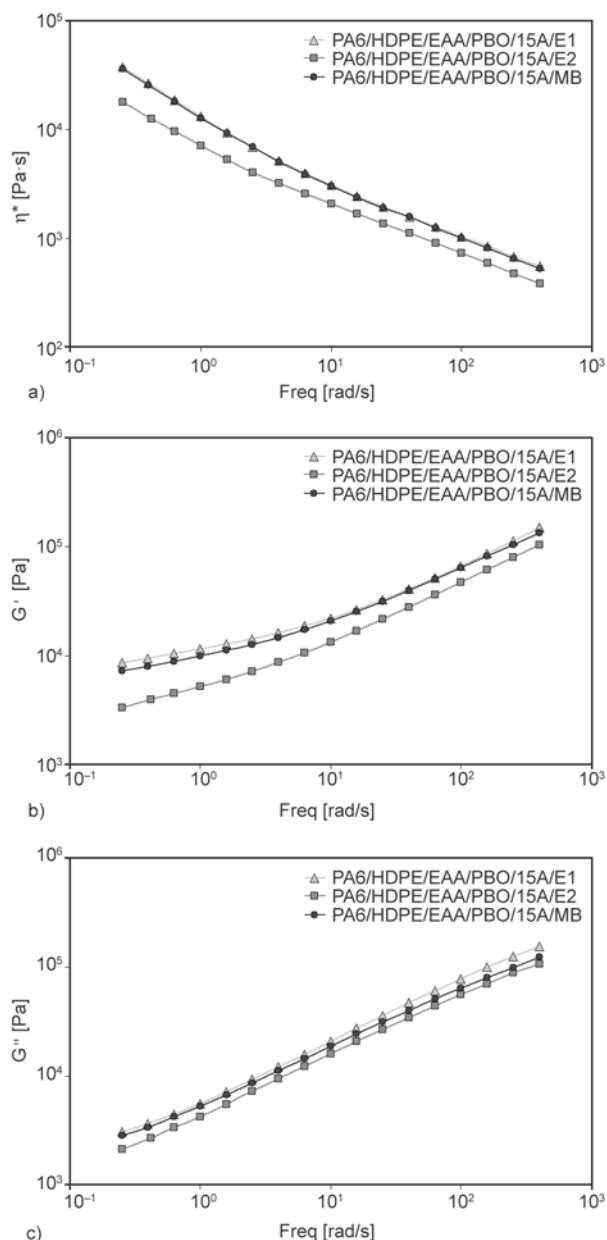
Figure 5. Complex viscosity (a), storage modulus (b) and the loss modulus (c) as a function of frequency of blend compatibilized with EAA prepared by single extrusion (E1), re-extrusion (E2) and extrusion with a masterbatch (MB)
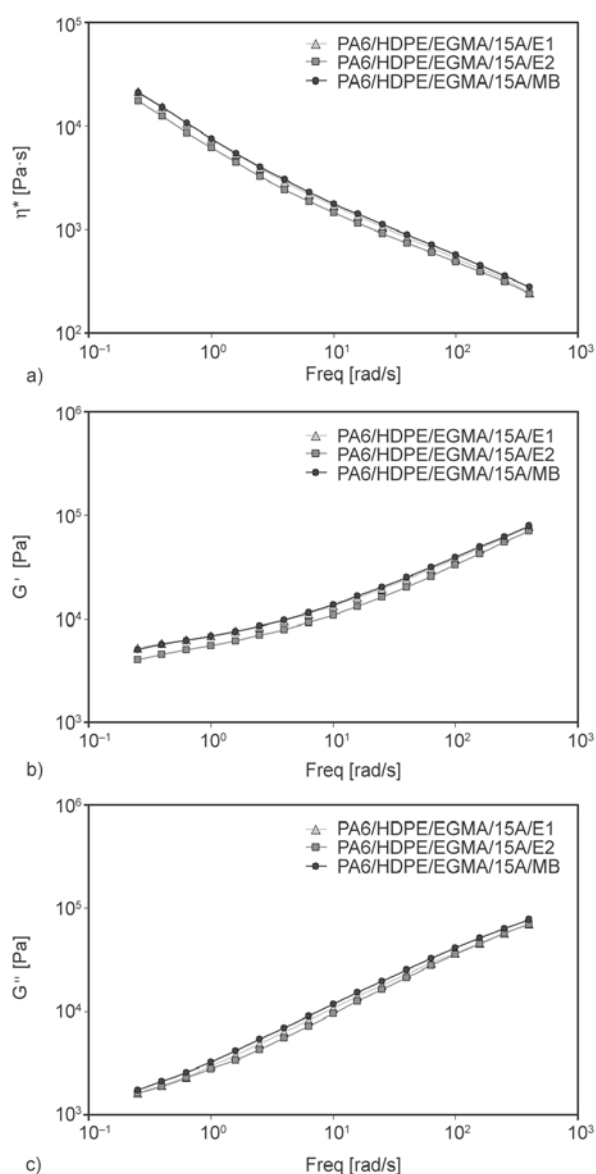
HDPE, PA6 and the clay are exposed to high temperatures and mechanical stresses for a second time. According to our previous results, the degradation products of the clay can be responsible of a marked deactivation of the compatibilizing system [26, 27]. The decrease of the compatibilizing action given by EAA/PBO induces a lower phase adhesion and, consequently, a lower melt viscosity. For MB materials, actually, this phenomenon is less marked and the double processing of the clay has fewer consequences reasonably because the masterbatch prepa-
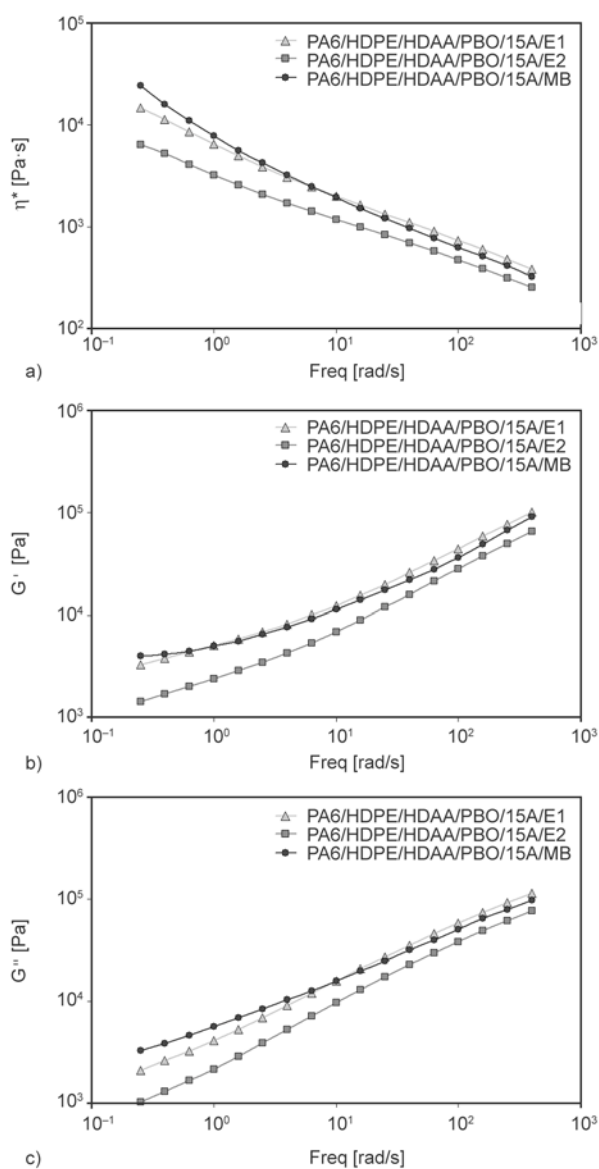
Figure 6. Complex viscosity (a), storage modulus (b) and the loss modulus (c) as a function of frequency of blend compatibilized with HDAA prepared by single extrusion (E1), re-extrusion (E2) and extrusion with a masterbatch (MB)

Figure 7. Complex viscosity (a), storage modulus (b) and the loss modulus (c) as a function of frequency of blend compatibilized with EGMA prepared by single extrusion (E1), re-extrusion (E2) and extrusion with a masterbatch (MB)

ration is carried out at 180°C, thus reducing the potential degradation effects on the clay after this step. Similar considerations can be done for the systems containing HDAA/PBO, Figure 6, and EGMA, Figure 7, even if in this latter case the reduction of viscosity is less relevant reasonably because of a minor compatibilizing effect of this agent and a lower antagonistic effect with the clay degradation products, confirming previous findings [26].

The analysis of the storage and loss moduli show that, for the EAA/PBO compatibilized blends, Figure 5, the differences in the rheological behaviour can be mainly attributed to the conservative compo-

nent, G', as the dissipative component, G'', remains practically unaltered for E1, E2 and MB materials. This is not true for the HDAA containing materials, Figure 6 as both G' and G'' significantly change comparing E1/MB materials with E2. EGMA containing blends, finally, Figure 7, show very small differences in G' and G'', thus corroborating the hypothesis of a bland activity of this compound as compatibilizing agent.

3.5. Mechanical characterization

In Table 4 it is reported the elastic modulus, E, the tensile stress, TS, the elongation at break, EB and

Table 4. Elastic modulus (*E*), tensile stress (*TS*), elongation at break (*EB*) and impact strength (*IS*) of compatibilized blends prepared by single extrusion (E1), re-extrusion (E2) and extrusion with a masterbatch (MB). The samples were prepared by compression moulding.

Sample	E [MPa]	TS [MPa]	EB [%]	IS [J/m]
PA6/HDPE/EAA/PBO/15A/E1	1283±32	23.6±0.3	3.1±0.1	24.0±1.0
PA6/HDPE/EAA/PBO/15A/E2	1348±39	23.4±0.4	3.4±0.2	28.5±0.9
PA6/HDPE/EAA/PBO/15A/MB	1452±43	23.8±0.3	4.0±0.2	33.3±1.1
PA6/HDPE/HDAA/PBO/15A/E1	1169±27	17.3±0.6	1.9±0.2	23.7±0.9
PA6/HDPE/HDAA/PBO/15A/E2	1229±33	21.6±0.4	2.4±0.1	30.3±1.0
PA6/HDPE/HDAA/PBO/15A/MB	1353±41	22.6±0.5	2.9±0.1	31.2±0.8
PA6/HDPE/EGMA/15A/E1	1173±28	23.3±0.8	5.0±0.3	28.3±0.7
PA6/HDPE/EGMA/15A/E2	1287±34	26.7±0.6	5.9±0.3	36.4±1.1
PA6/HDPE/EGMA/15A/MB	1297±28	27.3±0.7	7.5±0.4	42.0±1.3

the impact strength, *IS*, measured on compression moulded specimens of all the nanocomposites.

As regards all the compatibilized systems reprocessing (E2) induce an increase of all the properties for all the systems.

This improvement is in full agreement with the better blend morphology and with the improved clay distribution and intercalation after the second processing, as commented above. To go deeper inside this aspect, i.e. to investigate if the improvement of the mechanical properties was due to a better filler redistribution or to a finer polymer blend matrix morphology after reprocessing, unfilled materials were re-extruded and tested. The values of all the mechanical properties (here not reported for sake of brevity) do not show significant changes after the second processing for all the compatibilizing systems used, exception made for *EB* that shows a slight reduction. It can be therefore concluded that the improvement of the mechanical properties in the composites have to be attributed to the clay rather than to the polymer blend matrix.

Also the composites prepared using the compatibilizer-clay masterbatch show a general increase of the mechanical properties even if some specific comments must be given. The highest increase of Young's modulus can be found in the EAA containing system but the overall better improvement is found in the EGMA system. These results confirm that the pre-dispersion of the clay in the compatibilizer helps in achieving a further dispersion in the final material. Moreover, the differences in the performances of the different compatibilizers can be explained either with the different viscosity of the compatibilizers under the masterbatch preparation conditions. In particular, the lower the viscosity the lower the shear stress acting in the melt and the worse the dispersion. In this sense, as reported in EAA and EGMA show the highest viscosities and therefore it is reasonable to suppose that the initial dispersion of the clay in the masterbatch preparation step is more effective than that of HDAA [26]. Of course, a different affinity between the compatibilizer and the clay leading to different melt interactions between the two components could be also taken into account.

As regards the impact strength, Table 4, it can be observed the same trend already evidenced in the tensile properties. *IS* is increasing according to E1< E2<MB. Again, the highest increase are observed for EAA and especially for EGMA containing materials while when using HDAA this increment is definitely lower. These results confirm that, beyond the better dispersion of the clay, there is also an improved adhesion between the filler and the matrix that enhances the stress transmission between the phases and, consequently, reduces crack propagation.

4. Conclusions

We studied the influence of morphology achieved by different processing methods, on the rheological and mechanical properties of PA6/HDPE-clay nanocomposite blends in the presence of different compatibilizing systems. The XRD and TEM analysis showed that the re-extrusion improves slightly the morphology probably because to the supplementary stresses induced on the blend by the second processing allowing a further dispersion of the nanofiller with consequent higher intercalation level. A further improvement of the morphology, in terms of lower clay dimension and better dispersion, can be observed in the blends MB. These results can be explained considering that the preparation of the

compatibilizer-clay masterbatch may induce a certain initial intercalation/expansion of the clay that becomes more intense during the subsequent extrusion processing. The rheological characterization showed that the E2 blends have a lower viscosity in comparison with the respective E1 blends. This can be likely interpreted with degradation phenomena occurring during the second reprocessing. Indeed, in E2 blends, HDPE, PA6 and the clay are exposed to high temperatures and mechanical stresses for a second time. On the contrary, the MB blends exhibited values of viscosity similar to E1 blends. This can be explained considering that the masterbatch preparation is carried out at 180°C, thus reducing the potential degradation effects on the clay after this step. The results of the mechanical tests showed that reprocessing (E2) induced an increase of all the properties for all the three systems. This improvement is in full agreement with the better blend morphology and with the improved clay distribution and intercalation after the second processing. A further general increase of the mechanical properties was showed by the blends MB. These results confirm that the pre-dispersion of the clay in the compatibilizer helps in achieving a further dispersion in the final material.

Acknowledgements

References

[1] Nazari T., Garmabi H.: Effect of organoclays on the rheological and morphological properties of poly (acrylonitrile-butadiene-styrene)/poly(methyl methacrylate)/clay nanocomposites. Polymer Composites, **33**, 1893–1902 (2012).
DOI: 10.1002/pc.22329

[2] Yu Z., Yin J., Yan S., Xie Y., Ma J., Chen X.: Biodegradable poly(L-lactide)/poly(ε-caprolactone)-modified montmorillonite nanocomposites: Preparation and characterization. Polymer, **48**, 6439–6447 (2007).
DOI: 10.1016/j.polymer.2007.07.024

[3] Bhatia A., Gupta R. K., Bhattacharya S. N., Choi H. J.: An investigation of melt rheology and thermal stability of poly(lactic acid)/poly(butylene succinate) nanocomposites. Journal of Applied Polymer Science, **114**, 2837–2847 (2009).
DOI: 10.1002/app.30933

[4] Martín Z., Jiménez I., Gómez M. Á., Ade H., Kilcoyne D. A.: Interfacial interactions in PP/MMT/SEBS nanocomposites. Macromolecules, **43**, 448–453 (2010).
DOI: 10.1021/ma901952p

[5] Praveen S., Chattopadhyay P. K., Jayendran S., Chakraborty B. C., Chattopadhyay S.: Effect of rubber matrix type on the morphology and reinforcement effects in carbon black-nanoclay hybrid composites – A comparative assessment. Polymer Composites, **31**, 97–104 (2010).
DOI: 10.1002/pc.20772

[6] Naderi G., Lafleur P. G., Dubois C.: The influence of matrix viscosity and composition on the morphology, rheology, and mechanical properties of thermoplastic elastomer nanocomposites based on EPDM/PP. Polymer Composites, **29**, 1301–1309 (2008).
DOI: 10.1002/pc.20495

[7] Chow W. S., Mohd Ishak Z. A., Karger-Kocsis J., Apostolov A. A., Ishiaku U. S.: Compatibilizing effect of maleated polypropylene on the mechanical properties and morphology of injection molded polyamide 6/polypropylene/organoclay nanocomposites. Polymer, **44**, 7427–7440 (2003).
DOI: 10.1016/j.polymer.2003.09.006

[8] Calcagno C. I. W., Mariani C. M., Teixeira S. R., Mauler R. S.: The role of the MMT on the morphology and mechanical properties of the PP/PET blends. Composites Science and Technology, **68**, 2193–2200 (2008).
DOI: 10.1016/j.compscitech.2008.03.012

[9] Hong J. S., Namkung H., Ahn K. H., Lee S. J., Kim C.: The role of organically modified layered silicate in the breakup and coalescence of droplets in PBT/PE blends. Polymer, **47**, 3967–3975 (2006).
DOI: 10.1016/j.polymer.2006.03.077

[10] Paul D. R., Bucknall C. B.: Polymer blends, formulation. Wiley, New York (2000).

[11] La Mantia F. P., Scaffaro R., Colletti C., Dimitrova T., Magagnini P., Paci M., Filippi S.: Oxazoline functionalization of polyethylenes and their blends with polyamides and polyesters. Macromolecular Symposia, **176**, 265–278 (2001).
DOI: 10.1002/1521-3900(200112)176:1<265::AID-MASY265>3.0.CO;2-I

[12] Liu X., La Mantia F. P., Scaffaro R.: Oxazoline-containing compatibilizers for polyamide/SAN and polyamide/ABS blends. Journal of Applied Polymer Science, **86**, 449–455 (2002).
DOI: 10.1002/app.11002

[13] Scaffaro R., La Mantia F. P., Canfora L., Polacco G., Filippi S., Magagnini P.: Reactive compatibilization of PA6/LDPE blends with an ethylene–acrylic acid copolymer and a low molar mass bis-oxazoline. Polymer, **44**, 6951–6957 (2003).
DOI: 10.1016/j.polymer.2003.06.001

[14] Utracki L. A.: Polymer blends handbook. Kluwer, Dordrecht (2003).

[15] Scaffaro R., Botta L., La Mantia F. P., Magagnini P., Acierno D., Gleria M., Bertani R.: Effect of adding new phosphazene compounds to poly(butylene terephthalate)/polyamide blends. I: Preliminary study in a batch mixer. Polymer Degradation and Stability, **90**, 234–243 (2005).
DOI: 10.1016/j.polymdegradstab.2005.03.019

[16] Scaffaro R., Botta L., La Mantia F. P., Gleria M., Bertani R., Samperi F., Scaltro G.: Effect of adding new phosphazene compounds to poly(butylene terephthalate)/polyamide blends. II: Effect of different polyamides on the properties of extruded samples. Polymer Degradation and Stability, **91**, 2265–2274 (2006).
DOI: 10.1016/j.polymdegradstab.2006.04.019

[17] Robeson L. M.: Polymer blends: A comprehensive review. Hanser, Munich (2007).

[18] Samperi F., Bazzano S., Battiato S., Scaffaro R., Botta L., Mistretta M. C., Bertani R., Milani R.: Reactions occurring during the melt mixing of nylon 6 and oxazoline–cyclophosphazene units. Macromolecules, **42**, 5579–5592 (2009).
DOI: 10.1021/ma9008466

[19] Filippone G., Dintcheva N. Tz., La Mantia F. P., Acierno D.: Selective localization of organoclay and effects on the morphology and mechanical properties of LDPE/PA11 blends with distributed and co-continuous morphology. Journal of Polymer Science Part B: Polymer Physics, **48**, 600–609 (2010).
DOI: 10.1002/polb.21928

[20] Ophir A., Dotan A., Belinsky I., Kenig S.: Barrier and mechanical properties of nanocomposites based on polymer blends and organoclays. Journal of Applied Polymer Science, **116**, 72–83 (2010).
DOI: 10.1002/app.31285

[21] Contreras V., Cafiero M., Da Silva S., Rosales C., Perera R., Matos M.: Characterization and tensile properties of ternary blends with PA-6 nanocomposites. Polymer Engineering and Science, **46**, 1111–1120 (2006).
DOI: 10.1002/pen.20572

[22] Sharif-Pakdaman A., Morshedian J., Jahani Y.: Effect of organoclay and silane grafting of polyethylene on morphology, barriority, and rheological properties of HDPE/PA6 blends. Journal of Applied Polymer Science, **127**, 1211–1220 (2013).
DOI: 10.1002/app.37974

[23] Yoo Y., Park C., Lee S-G., Choi K-Y., Kim D. S., Lee J. H.: Influence of addition of organoclays on morphologies in nylon 6/LLDPE blends. Macromolecular Chemistry and Physics, **206**, 878–884 (2005).
DOI: 10.1002/macp.200400526

[24] Fang Z., Xu Y., Tong L.: Effect of clay on the morphology of binary blends of polyamide 6 with high density polyethylene and HDPE-*graft*-acrylic acid. Polymer Engineering and Science, **47**, 551–559 (2007).
DOI: 10.1002/pen.20675

[25] Scaffaro R., Mistretta M. C., La Mantia F. P.: Compatibilized polyamide 6/polyethylene blend–clay nanocomposites: Effect of the degradation and stabilization of the clay modifier. Polymer Degradation and Stability, **93**, 1267–1274 (2008).
DOI: 10.1016/j.polymdegradstab.2008.04.008

[26] Scaffaro R., Botta L., Mistretta M. C., La Mantia F. P.: Preparation and characterization of polyamide 6/polyethylene blend-clay nanocomposites in the presence of compatibilisers and stabilizing system. Polymer Degradation and Stability, **95**, 2547–2554 (2010).
DOI: 10.1016/j.polymdegradstab.2010.07.029

[27] Scaffaro R., Mistretta M. C., La Mantia F. P., Frache A.: Effect of heating of organo-montmorillonites under different atmospheres. Applied Clay Science, **45**, 185–193 (2009).
DOI: 10.1016/j.clay.2009.06.002

[28] Scaffaro R., Botta L., Frache A., Bellucci F.: Thermo-oxidative ageing of an organo-modified clay and effects on the properties of PA6 based nanocomposites. Thermochimica Acta, **552**, 37–45 (2013).
DOI: 10.1016/j.tca.2012.11.007

[29] Goitisolo I., Eguiazábal J. I., Nazábal J.: Effects of reprocessing on the structure and properties of polyamide 6 nanocomposites. Polymer Degradation and Stability, **93**, 1747–1752 (2008).
DOI: 10.1016/j.polymdegradstab.2008.07.030

[30] Karahaliou E-K., Tarantili P. A.: Preparation of poly(acrylonitrile–butadiene–styrene)/montmorillonite nanocomposites and degradation studies during extrusion reprocessing. Journal of Applied Polymer Science, **113**, 2271–2281 (2009).
DOI: 10.1002/app.30158

[31] Abdel Gawad A., Esawi A. M. K., Ramadan A. R.: Structure and properties of nylon 6–clay nanocomposites: effect of temperature and reprocessing. Journal of Materials Science, **45**, 6677–6684 (2010).
DOI: 10.1007/s10853-010-4760-5

[32] Russo G. M., Nicolais V., Di Maio L., Montesano S., Incarnato L.: Rheological and mechanical properties of nylon 6 nanocomposites submitted to reprocessing with single and twin screw extruders. Polymer Degradation and Stability, **92**, 1925–1933 (2007).
DOI: 10.1016/j.polymdegradstab.2007.06.010

[33] Touati N., Kaci M., Bruzaud S., Grohens Y.: The effects of reprocessing cycles on the structure and properties of isotactic polypropylene/Cloisite 15A nanocomposites. Polymer Degradation and Stability, **96**, 1064–1073 (2011).
DOI: 10.1016/j.polymdegradstab.2011.03.015

[34] Remili C., Kaci M., Benhamida A., Bruzaud S., Grohens Y.: The effects of reprocessing cycles on the structure and properties of polystyrene/Cloisite 15A nanocomposites. Polymer Degradation and Stability, **96**, 1489–1496 (2011).
DOI: 10.1016/j.polymdegradstab.2011.05.005

[35] Scaffaro R., Botta L., Ceraulo M., La Mantia F. P.: Effect of kind and content of organo-modified clay on properties of PET nanocomposites. Journal of Applied Polymer Science, **122**, 384–392 (2011). DOI: 10.1002/app.34087

[36] Botta L., Scaffaro R., La Mantia F. P., Dintcheva N. Tz.: Effect of different matrices and nanofillers on the rheological behavior of polymer-clay nanocomposites. Journal of Polymer Science Part B: Polymer Physics, **48**, 344–355 (2010). DOI: 10.1002/polb.21896

[37] Botta L., La Mantia F. P., Dintcheva N. Tz., Scaffaro R.: Rheological response of polyethylene/clay nanocomposites to annealing treatment. Macromolecular Chemistry and Physics, **208**, 2533–2541 (2007). DOI: 10.1002/macp.200700241

[38] Shah R. K., Paul D. R.: Nylon 6 nanocomposites prepared by a melt mixing masterbatch process. Polymer, **45**, 2991–3000 (2004). DOI: 10.1016/j.polymer.2004.02.058

[39] Filippone G., Dintcheva N. Tz., Acierno D., La Mantia F. P.: The role of organoclay in promoting co-continuous morphology in high-density poly(ethylene)/poly(amide) 6 blends. Polymer, **19**, 1312–1322 (2008). DOI: 10.1016/j.polymer.2008.01.045